

Development of 3D Printed Scaffolds for Bone Regeneration

Wegdan Hamed Nasser Hasha



This thesis is submitted in partial fulfillment of the requirements for the degree of Master of
Philosophy in Oral Sciences at the University of Bergen

Center for International Health

Department of Clinical Dentistry

Faculty of Medicine and Dentistry

University of Bergen, Norway

2016

Development of 3D Printed Scaffolds for Bone Regeneration

Wegdan Hamed Nasser Hasha

This thesis is submitted in partial fulfilment of the requirements for the degree of
Master of Philosophy in Oral Sciences at the University of Bergen.

Center for International Health

Department of Clinical Dentistry

Faculty of Medicine and Dentistry

University of Bergen, Norway

2016

Abstract

The 3D printing process can produce bioengineered scaffolds with a 100% interconnected porous structure layer-by-layer with the help of computer-aided design. In this study we utilized a 3D bio plotter system to fabricate 3D interconnected porous scaffolds for bone tissue engineering. Poly (L-lactide-co-caprolactone (PLCL)) was selected to fabricate the scaffold due to its biocompatibility and printability. Two scaffolds were produced for comparative study with a layer rotation of 45° and 90° and a distance of either 1000 µm or 1200 µm between the printed fibers.

Micro computed tomography (µ-CT) was utilized to study the interconnected porous structure of the scaffolds. Protein adsorption on the surface of the scaffolds was examined using a protein assay kit. Human osteoblast-like cells (HOB) were seeded onto the two different scaffolds and cellular activities (attachment, morphology, and proliferation) were investigated using scanning electron microscopy (SEM), live/dead stain, lactate dehydrogenase enzyme (LDH), and methylthiazol tetrazolium (MTT). Gene expression of apoptotic (Bax and Bcl2) and osteogenic markers (ALP and OC) were investigated by qRT-PCR. The µ-CT results confirmed the open porous structure of the two scaffolds and no significant difference was found in protein adsorption between the two designs. SEM, LDH and MTT analysis confirmed that HOB cells adhered, spread and proliferated well on both scaffolds. The qRT-PCR analysis showed that cells seeded on the scaffold with 1200 µm between the fibers expressed higher mRNA levels of Bcl2 (day 1, 3, 7 and 14), ALP and OC than cells seeded on the scaffold with 1000 µm between fibers (day 14).

In conclusion, the newly designed 3D printed scaffolds are biocompatible with HOBs, and no adverse effect on cell attachment and proliferation was seen. Rather, enhanced osteoblast proliferation and differentiation were seen using the scaffold with 1200 µm

between the printed fibers. Therefore, 1200 3D printed poly (L-lactide-co-caprolactone) scaffolds may be suitable candidates for bone regeneration.

Contents

Acronyms and Abbreviations	7
Acknowledgements	9
Summary	11
1. Introduction	13
1.1. Tissue Engineering and the concept of tissue engineering	13
1.2. Bone tissue engineering (BTE).....	14
1.3. Cells for tissue engineering	16
1.4. Growth factors in bone regeneration	16
1.5. Scaffolds in bone tissue engineering	17
1.6. Cell/tissue-scaffold interactions	20
2. Aims	21
3. Materials and Methods	22
3.1. Scaffold design and fabrication	22
3.1.1. Materials	22
3.1.2. Scaffold design	22
3.1.3. Scaffold fabrication	23
3.1.4. Sterilization	25
3.2. Characterization of scaffold	25
3.2.1. X-ray micro-computed tomography	25
3.2.2. Protein adsorption.....	25
3.3. Cell cultures and scaffold seeding	26
3.3.1. Scanning electron microscopy (SEM).....	27
3.3.2. Live and Dead assay (L&D).....	28
3.3.3. Lactate dehydrogenase assay (LDH).....	28
3.3.4. Methylthiazol tetrazolium (MTT) assay.....	29
3.4. QRT-PCR gene expression	29
3.5. Statistical Analysis	30
4. Results	31
4.1. Scaffold fabrication:	31
4.2. Characterization of scaffolds	31
4.2.1. Microcomputed tomography analysis (μ CT)	31
4.2.2. Protein adsorption.....	34

4.3. Cellular activities.....	35
4.3.1. Cell proliferation	35
4.3.2. Cell morphology and cell attachment	37
4.3.3. Cell viability Live / dead assay	38
4.3.4. LDH assay	38
4.3.5. MTT assay	39
4.4. qRT-PCR	40
4.4.1. Apoptosis.....	40
4.4.2. Bone markers.....	40
5. Discussion	42
6. Conclusions	47
7. References	48

Acronyms and Abbreviations

2D	2-dimentional
3D	3-dimensional
3DP	3-dimensional plotting
AB	Antibiotics
ALP	Alkaline phosphatase
α -MEM	Minimum essential medium, alpha modification
BTE	Bone tissue engineering
DMEM	Dulbecco's modified Eagle's medium
ECM	Extra cellular Matrix
FBS	Fetal Bovine Serum
FDA	Food and Drug Administration
$2^{-\Delta\Delta Ct}$ method	Comparative CT method for relative quantification
cDNA	Complementary deoxyribonucleic Acid
GAPDH	Glyceraldehyde-3-phosphate dehydrogenase
HOBs	Human osteoblast-like cells
L929	Mouse fibroblast cell line
LDH	Lactic Dehydrogenase Based

L&D	Live and Dead
μ CT	Microcomputed tomography
mRNA	Messenger ribonucleic acid
MTT	Methylthiazol tetrazolium
OC	Osteocalcin
PBS	Phosphate buffered saline
PLCL	Poly (L-lactide- <i>co</i> -caprolactone)
SEM	Scanning electron microscopy
qRT-PCR	Quantitative Reverse Transcription-Polymerase Chain
TE	Tissue Engineering

Acknowledgements

This thesis was supported by The Center for International Health (CIH) and The Center for Clinical Dental Research-Department of Clinical Dentistry, Faculty of Medicine and Dentistry, University of Bergen, Norway in the period from 2014 to 2016. This study was approved by Ethics Committee of the University of Bergen. Many people encouraged me to achieve this important milestone in my life.

First and foremost, I am deeply indebted to my supervisor's **Postdoctoral fellow Shaza Idris** for excellent supervision, for guidance, and for patience and encouragement throughout the studies, especially during the most frustrating times, and I am also grateful for my co-supervisor **Professor Kamal Mustafa**.

I would like to express my gratitude to UiB for giving me this precious opportunity to get into research. I also acknowledge the Norwegian State Educational Loan Fund (Statens Lånekasse) for affording me the funds for this work. I would like to thank the teaching and administrative staff at CIH and special thanks to Linda Karin Forshaw for her energetic efforts and limitless assistance and patience.

Thanks to our main collaborators *Associate Professor Anna Finne-Wistrand*, at the Department of Fiber and Polymer Technology, KTH, Stockholm and the wonderful researcher Yang Sun Who produced the two different types of scaffold, at Center for Clinical Dental Research, Faculty of Medicine and Dentistry.

I would also like to thank the staff and PhD students at The Center of Clinical Dental Research, for creating such a positive working environment: (*Siren Hammer Ostvold, Randi Sundfjord*, from each of you I have learnt new about research and I continue to learn every day many things.

I sincerely thank Dr. Michele Fox for the excellent revision of the manuscripts and the thesis for English style and grammar, correcting both and offering suggestions for improvement. Special thanks to PhD students Ahmad Rashad Elsebahy and Niyaz Abdulbaqi and all my Sudanese friends especially Salwa Mustafa and Mohammed Yassin at IKO, UIB, Tissue Engineering Group at Center for Clinical Dental Research at IKO, UIB, for all the amazing and enjoyable times we have shared that make me happy.

Finally, I would like to express my love and appreciation for my family: for their great love and support, my mother for her full love, brothers (Majid and Mohammed), sisters (Donya, Ehab and Raghed), for believing in me and limitless love. Geed My lovely daughter, Ahmed my polite son, Faisal my cute baby and for the special person in my life the dearest and sweets husband Alaa Ali for the positive support and encouragement which empowered me to complete this work and change all my life.

Thank you;

Bergen, June, 2016

Wegdan Hamed Nasser Hasha

Summary

Organ failure and dysfunction caused by damaged or diseased tissue is increasing due to trauma, sickness and the aging population, all of which can drastically affect the quality of life. The current need for organ or tissue replacement is increasing. Bone tissue engineering has therefore been of increasing interest recently as a potential alternative to the use of bone grafts as a way to heal bone defects and restore lost bone. That is, treatment of bone defects via bone tissue engineering now aims to encourage new, functional bone regeneration by combining three main components: a rich source of osteoprogenitor cells, biocompatible scaffolds favorable to maintenance of cell function and osteoinductive growth factors.

Biodegradable 3D printed scaffolds were used in the present study to provide a microenvironment that supports cell attachment, proliferation and differentiation, thus inducing functional bone tissues. The specific aim of the study was to evaluate the effect of the distance between the printed fibers of the scaffold on these biological responses. Poly (LLA-*co*-CL) scaffolds were generated for the study and printed with a distance of either 1000 μm or 1200 μm between the fibers.

The scaffolds were characterized and seeded with human osteoblast-like cells (HOBs) to investigate the cells' ability to attach, proliferate and differentiate on the two different scaffolds.

The results showed that the 3D scaffolds are not cytotoxic, are biocompatible and do not have an adverse effect on the attachment and proliferation of HOBs *in vitro*. Moreover, the 1200 μm scaffold enhanced proliferation and expression of osteogenic markers by HOBs compared to the 1000 μm scaffold *in vitro*. Therefore, the 1200 μm 3D printed scaffold appear to be appropriate carriers for bone engineering investigations and regeneration.

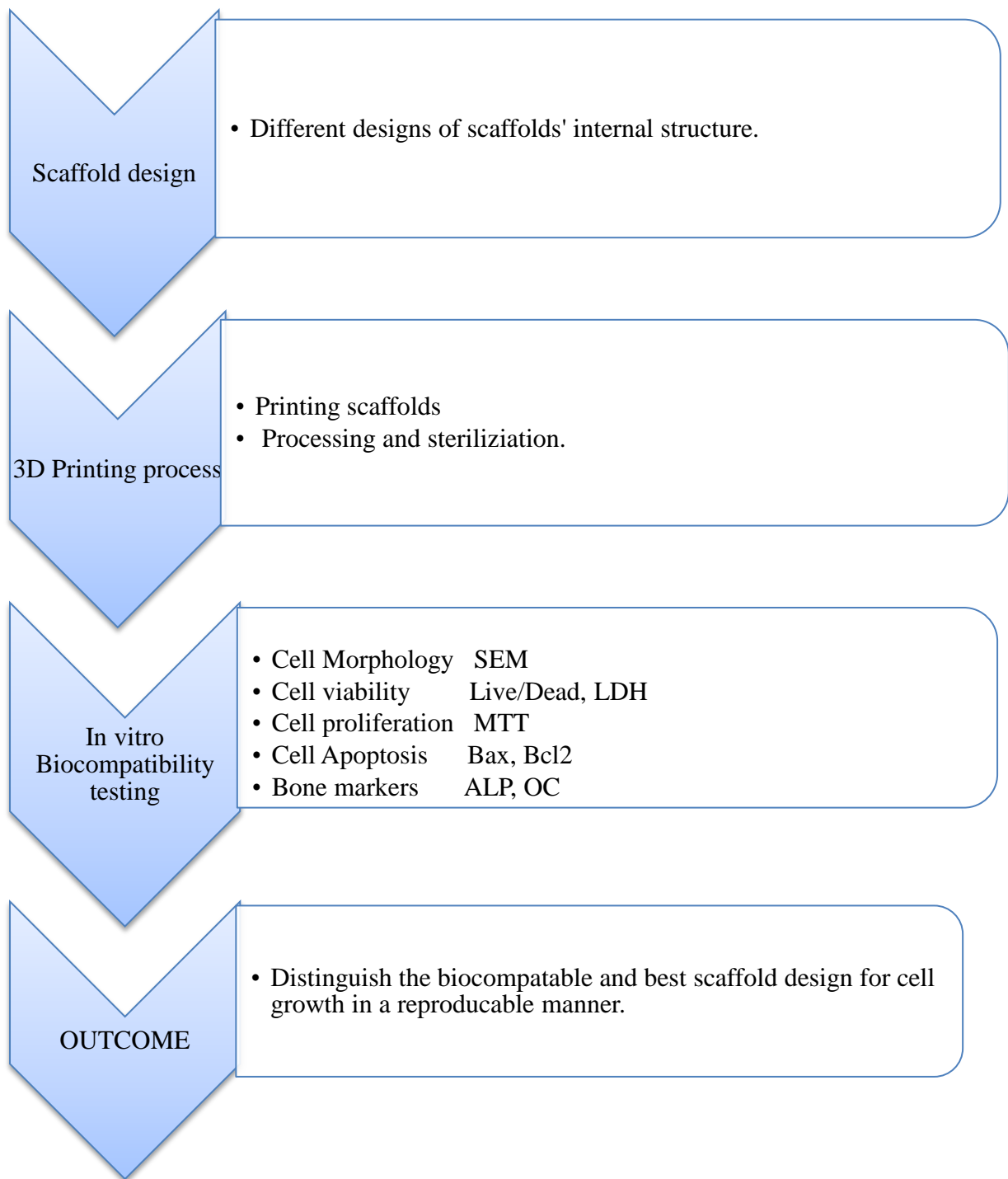


Figure 1. Flow chart describing the summary of materials and methods being used

1. Introduction

1.1. Tissue Engineering and the concept of tissue engineering

Tissue engineering (TE) was defined by Langer and Vacanti in 1993 as “an inter disciplinary field of research that applies the principles of engineering and life sciences towards the development of biological substitutes that restore, maintain, or improve tissue function" (1). TE requires a rich source of osteoprogenitor cells to repair defective bone tissue and a scaffold to encourage the attachment of the cells in combination with a specific growth factor or factors (signaling molecules) (1, 2). The scaffold should degrade in time when the tissue has matured, while permitting the newly forming tissue to function during the period of regeneration (3).

As the result of substantial collaborative efforts between scientists, engineers, and surgeons TE is developing rapidly as a potential alternative for human organ and tissue transplant (4), especially in the area of engineered bone grafts to enhance bone repair and regeneration (5). New advances in the field of bone tissue engineering have involved the use of biocompatible scaffolds, new perinatal multipotent cells, and the suitable cellular stimulation with growth factors and signaling molecules (6).

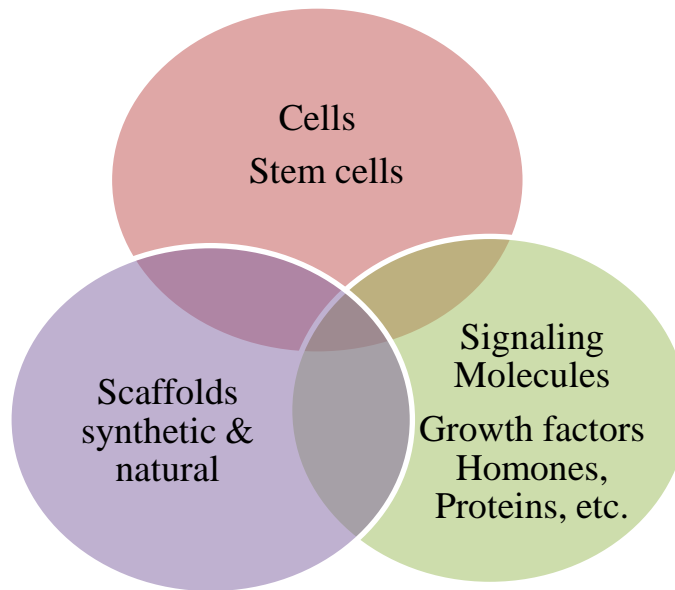


Figure 2. The three major components of bone tissue engineering

1.2. Bone tissue engineering (BTE)

By 2020 the worldwide prevalence of bone disorders is expected to double, especially in populations where aging is coupled with increasing obesity, and poor physical activity (7). Rehabilitation of bone defects as a result of congenital defects, trauma and tumor presents a clinical challenge using current therapeutic approaches (8). Biological grafts can be subdivided into autografts (bone tissue from the same individual), allografts (bone tissue from another individual of the same species), and xenografts (bone tissue from other species) (9, 10). Bone tissue engineering is therefore a field of rapidly growing interest as it has been suggested as an alternative to the current use of autologous and allogenic bone grafts, which have the drawbacks of limited supply, difficulty in shaping and potential for disease transmission (7). Bone tissue engineering thus appears to be a promising approach to improve human health through prevention of disease and restoration functions of healthy tissue (11).

The objectives of bone tissue engineering are to induce new functional bone through the synergistic combination of cells, growth factors and scaffolds (7). Bone tissue engineering is based on the current understanding of bone mechanics, structure, and tissue formation as it pertains to stimulating new functional bone tissues (7). During the next 25 years bone tissue engineering is expected to have a significant effect on dental and medical practice (12).

Scaffolds suitable for bone tissue engineering should fulfill certain basic requirements, i.e.: stimulation of progenitor cells to differentiate into cells of the osteoblastic lineage (Osteoinduction), encourages bone growth and the ingrowth of surrounding tissue (Osteoconduction) (13).

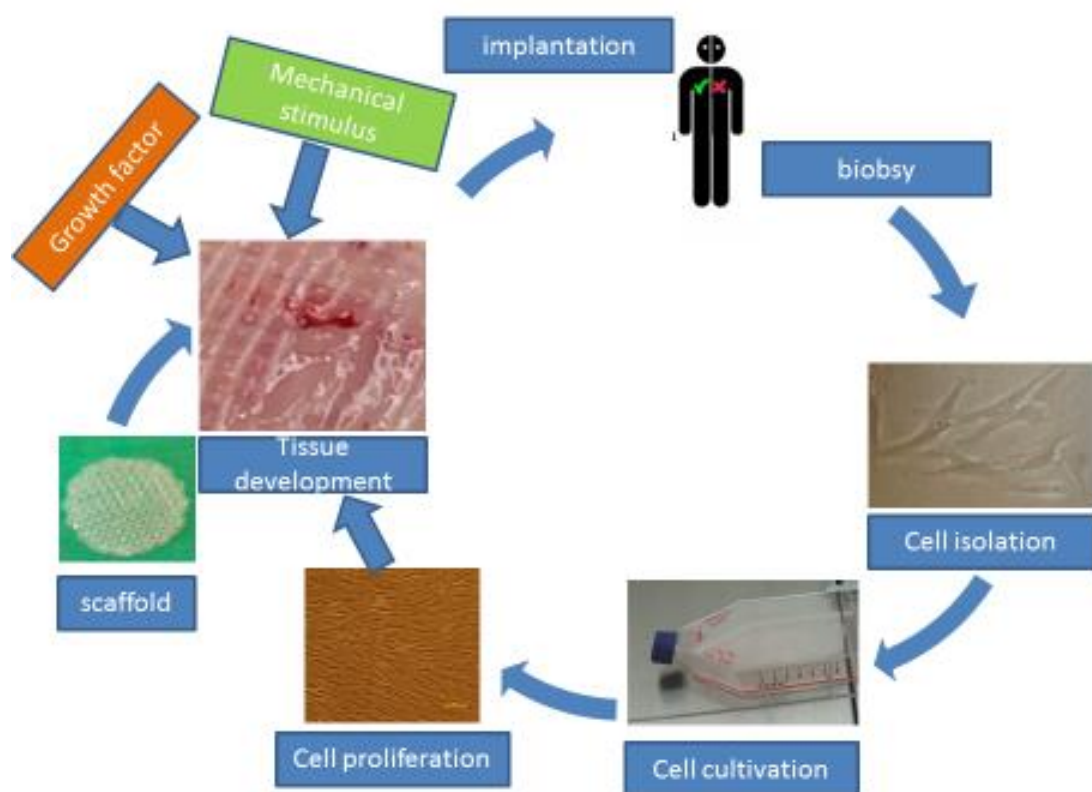


Figure3. Cells isolated from a biopsy, seeded *in vitro* on an appropriate scaffold (provisional ECM) and permitted to develop new tissue *in vitro* and *in vivo*.

1.3. Cells for tissue engineering

Both hematopoietic stem cells that produce cells of all hematopoietic lineages and human mesenchymal stem cells (hMSC) are found in adult human bone marrow (14). Mesenchymal stem cells (MSC) are potentially able to differentiate into multiple cell lineages *in vitro*, or *in vivo*, and have great capacity for self-renewal, leading to tissue regeneration as a basic part of the concept of TE. MSC have been shown to have the ability to differentiate into osteocytes, chondrocytes, myocytes and neurons *in vitro* and *in vivo* (2, 15, 16). MSC are mainly found in the bone marrow but can also be isolated from other tissue sources (17, 18).

Osteoblasts synthesize and secrete alkaline phosphatase (ALP), collagen type 1, and other noncollagenous extracellular bone matrix proteins such as osteocalcin (OC) and osteopontin. ALP plays an important role in the mineralization of the bone, while OC plays an important role in the ossification process of bone formation, making all of these useful markers of the various stages of osteogenesis, from cell proliferation and matrix synthesis to matrix mineralization (19).

1.4. Growth factors in bone regeneration

Growth factors are cytokines secreted by different types of cells and function as signaling molecules. They promote and/or prevent proliferation and differentiation of the cell (2). Thus, they are essential for tissue formation. Several growth factors are expressed and have reasonable effects on and during bone formation, such as fibroblast growth factor (FGF), bone morphogenetic proteins (BMPs), insulin-like growth factor (IGF), transforming growth factor β (TGF- β), platelet-derived growth factor (PDGF) and vascular epithelium growth factors (VEGF) (20).

1.5. Scaffolds in bone tissue engineering

A scaffold is a three-dimensional (3D) template for initial cell adhesion, proliferation and tissue regeneration (21-24). As reported by Hutmacher (24) the ideal scaffold for TE should be well integrated in the host's tissue with no immunological response. Moreover, it should have appropriate surface properties for cell attachment, proliferation and differentiation, and should have high porosity to facilitate transport of nutrients and metabolic waste. Scaffolds also require excellent biocompatibility, with controllable degradation and resorption rates to mimic normal tissue and organs, and good mechanical properties to match the rate of tissue growth *in vitro and in vivo* (24, 25). Biocompatibility is the ability of a device or biomaterial to perform as a substrate that supports appropriate cellular activity, or performs with the desired host response in order to optimize tissue regeneration (26). Cytotoxicity testing is generally performed to detect cell death or other serious negative effects on cellular functions at an early stage in the testing process. Cytotoxicity testing serves as a reproducible screening method, must be appropriate, and serve as a dependable test *in vitro* (27). Apoptotic activity is a sign of cell viability; both Bcl-2 (anti-apoptotic) and Bax (pro-apoptotic) are important regulators of apoptosis and play a crucial role in the regulation of cellular apoptosis. The balance between these genes therefore represents a measure of overall apoptotic activity (28).

Both natural and synthetic scaffold materials have been proposed for bone TE, including metals, ceramics and polymers (21). **Metals:** The good mechanical properties of metals make them excellent, if not the best choice, for implantable medical devices. Although metal has greater strength than the hard tissues of the body due to its stiffness, its lack of degradability in a biological environment is a drawback in scaffold fabrication (29, 30). **Ceramics:** include both naturally derived materials like coralline hydroxyl apatite (HA) and synthesized materials such as synthetic HA. The osteoinductive and osteoconductive properties of ceramics have led to their use in biomedical engineering and bone regeneration.

However, their low mechanical stability, brittleness, and stiffness that may give them increased strength relative to biologic hard tissue are significant disadvantages that prevent their use in regeneration of large bone defects (21, 29, 30). **Polymers:** are thermoplastics and have wide flexibility in physical properties, permitting them to be tailored to specific uses, and can be easily formed into desired shapes (30, 31).

There are two types of biodegradable scaffolds, natural and synthetic. The natural scaffolds are derived from natural sources such as collagen, fibrinogen, polysaccharides (starch, alginate, chitin/chitosan, hyaluronic) or proteins. These materials facilitate cell attachment, differentiation, migration, and tissue vascularization (21). The synthetic scaffold is more commonly used for tissue engineering and bone regeneration than the natural (32, 33).

There are many types of synthetic biodegradable polymers that have been used widely for TE. Poly (glycolic acid) (PGA) has high tensile strength with low solubility and can cause inflammatory reactions (33, 34). Poly (ϵ -caprolacton) (PCL) is highly compatible and has been examined as a material for controlled delivery of drugs due to its low degradation rate and high solubility in organic solvents (33, 35-37). Poly (lactic acid) (PLA) has desirable processing and mechanical properties and as a result of its low degradation rate is widely used as fixative devices in bone fracture, clinical products for drug delivery, sutures, guided tissue regeneration (in dental applications), and scaffolds for TE. Four different types of PLA are available but only poly (l-lactic acid) and poly (dl-lactic acid) have been widely investigated as biomaterials (33, 34). Scaffolds of poly (LLA) are biodegradable scaffolds that have been tested as alternatives to ceramic (36, 38). Poly (LLA) has been used in medical and orthopedic devices such as a bone fixator under the product names Fixsorb[®] (39), a resorbable suture Vicryl[®] and Phantom Suture Anchor[®] (40). It has been suggested that copolymers such as Poly (L-Lactide-co-caprolactone) {poly (LLA-co-CL)} are appropriate materials for enhancing bone tissue regeneration (35, 36, 41). These copolymers possess desirable

mechanical properties, good biocompatibility and degradability that can be used to produce scaffolds and increase function of cells attachment and proliferation (40, 42).

The synthetic scaffold can be designed using a variety of methods. The chemical/gas foaming method can be used to create porous structures in a continuous extrusion process, using a high pressure carbon dioxide gas, until saturation of the polymer mix, followed by a foaming process. This method is widely used industrially to produce closed cell thermoplastic foams, and a precise pore size distribution and porosity can be achieved that help cell infiltration, and provide suitable mechanical behavior (43). The solvent casting, particle/salt leaching method depends totally on the evaporation of the solvents. Using this technique is easy and there is no need for particular equipment during scaffolds fabrication, and there is therefore a low cost method. The freeze drying method has been used to fabricate scaffolds with high porosity and interconnectivity, depending on sublimation. The solution of dissolved polymer is frozen and the solvent is removed under high vacuum (44). However, each of these methods has some disadvantages; for example the use of highly toxic solvents, thin structure limitation, retention of particles in the scaffolds matrix, irregularity in pores size and shape, smaller pore size and long processing time (32, 45).

3D printed scaffolds are therefore being developed to overcome these problems (45). These scaffolds are designed for better blood vessel formation, ultimately leading to better bone formation (11) and can be used to build fully functional replacement for bones or organs (24). The demand for 3D printing is expected to increase due to their ability to make custom medical devices, produce scaffolds in a reproducible and controlled manner that improves mechanical properties, cell attachment and distribution (45, 46).

1.6. Cell/tissue-scaffold interactions

Optimizing cell-tissue scaffold material interactions are one of the main goals for tissue engineering. Cell-to-cell contact between cells and scaffold is required to stimulate the initial attachment, while cell spreading and cell growth may be influenced by surface texture (47), with a clear relationship between surface roughness of biomaterials and cell proliferation, adhesion, and morphology (48, 49). Further, the expression of adhesion proteins varies with respect to the surface roughness. (17, 47-49). 3D printed scaffolds are of interest as they can be processed into a variety of shapes and sizes for ideal attachment and growth. High porosity and high interconnectivity are essential to increase scaffold surface area for cell attachment and tissue ingrowth (50, 51), and 3D printed scaffolds can be made with different pore size, to accommodate the different pore size that may be required for different cells. Physical and chemical properties of the scaffold surface are also crucial for the cell-material interaction (52-55). 3D structure can be varied in many ways, as cell proliferation and distribution may be affected by many structural factors.

Recently, the use of 3D bio-plotter system has been used in tissue engineering (56). Different designs of the 3D scaffolds, different angles of rotation (45° and 90°), and scaffold characteristics have been shown to promote initial cell attachment and differentiation (46, 57, 58). Therefore, the aims of this study was to evaluate 3D printed scaffolds for bone tissue engineering (BTE) using two modified 3D printed scaffolds with different pore size (1000 µm and 1200 µm) and to investigate the effect of these scaffolds on cell viability, attachment, proliferation and differentiation.

2. Aims

The main objective of this study is:

To develop three dimensional (3D) printed scaffold in a reproducible and controlled manner.

The specific aim of this study is:

To investigate the effect of the 3D printed scaffolds developed on the following:

- Protein adsorption
- Cell attachment and morphology
- Cell viability and apoptosis
- Cell proliferation
- Osteogenic differentiation

3. Materials and Methods

3.1. Scaffold design and fabrication

3.1.1. Materials

Aliphatic thermoplastic poly (L-lactide-co-caprolactone) (PLCL, PURASORB® PLC 7015, CORBION, The Netherlands), synthesized from L-lactide and ϵ -caprolactone monomers with a molar ratio of 70/30 was used to produce the scaffolds. PLC 7015 has an inherent viscosity between 1.2-1.8 dl/g, and a maximum residual amount of tin of 100 ppm. The material was used as purchased.

3.1.2. Scaffold design

Scaffold dimensions chosen for the design were 11.5mm (diameter) x 2.5mm (thickness) in order to fit in a standard 48-well cell culture plate. The layer distance was 340 μ m in order to offer solid layer integration and adequate mechanical support. First, two designs with simple inner structures were printed. The first pattern had a rotational angle of 0/90 between each of the two layers and the second pattern had rotational angles of 0/45 degree (**Fig.4A and 4B**). These scaffolds were used to optimize both the printing process parameters and cell culture. Next, two modified 90°/45° rotational patterns were developed for this study. Pattern 1 had a strand distance of 1 mm between the first and second layers (L1/L2), and 0.71 mm between the third and fourth layers (L3/L4), while pattern 2 had a strand distance of 1.2 mm between L1/L2 and 0.86 mm between L3/L4. Every two connecting layers (L1/L2 or L3/L4) had a 90° cross rotation relative to each other. A rotation of 45° between L1/L2 and L3/L4 layers was plotted for an overlay on the top of cross points. Following the above method, a modified 90°/45° patterns with top-to-bottom cross point connections was built. This pattern has been

shown to have the capacity to sustain high compressive load force from the z axis (46) (Fig.5).

3.1.3. Scaffold fabrication

Scaffolds were produced by three-dimensional plotting method (3DP) method using a 3D Bioplotter system (4th generation, EnvisionTec GmbH, Germany). For each printing job, approximately 0.6 g of PLCL was loaded into a steel cartridge and heated to 175°C for 20 min until the polymer melted and stabilized. The cartridge was then heated up to 195°C for constant extrusion under a pressure of 6 bars. A 24G Luer lock stainless steel nozzle with an external diameter of 700 μm , and internal diameter 400 μm were used to extrude strands according to the design controlled by computer (Fig. 6). The pores of the two modified patterns of 3D printed scaffolds (1000 μm and 1200 μm) are investigated using the LEICA M205C microscope (Leica, Germany).

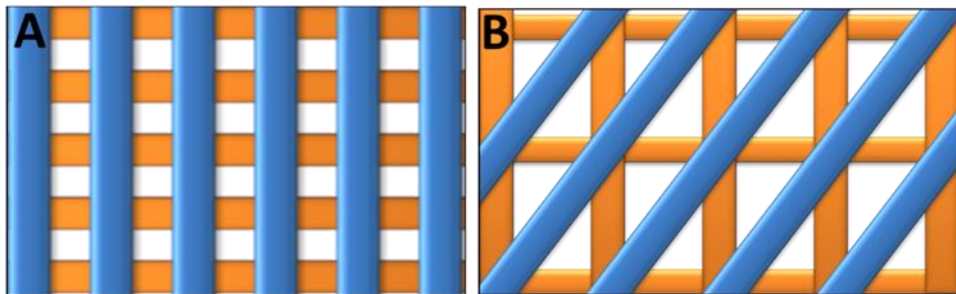


Figure 4. Drawing of a two designs with rotational angles of 0–90 (A) and 0–45 (B) in double layers.

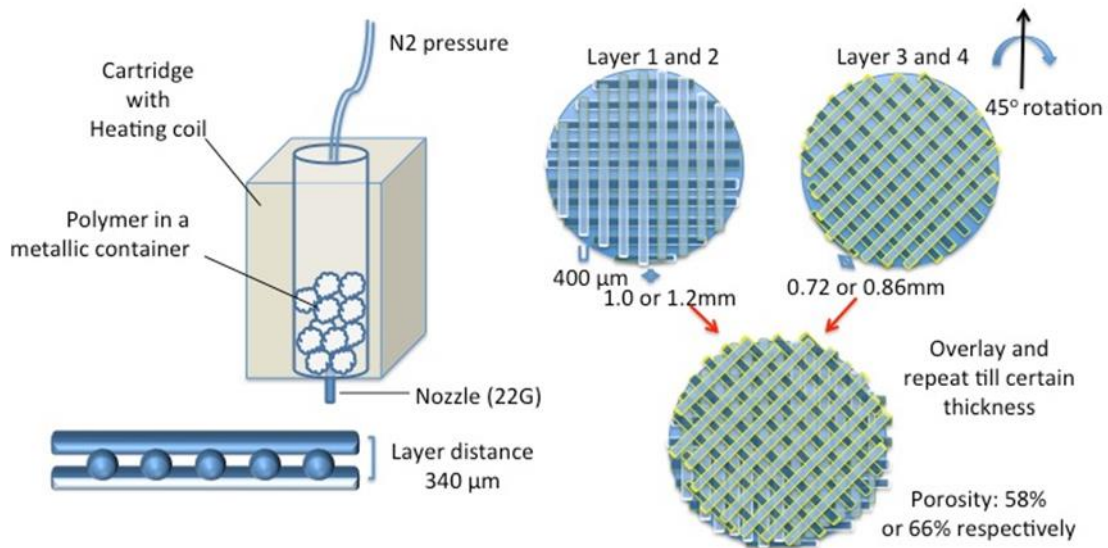


Figure 5. Scheme of plotting and scaffold design.

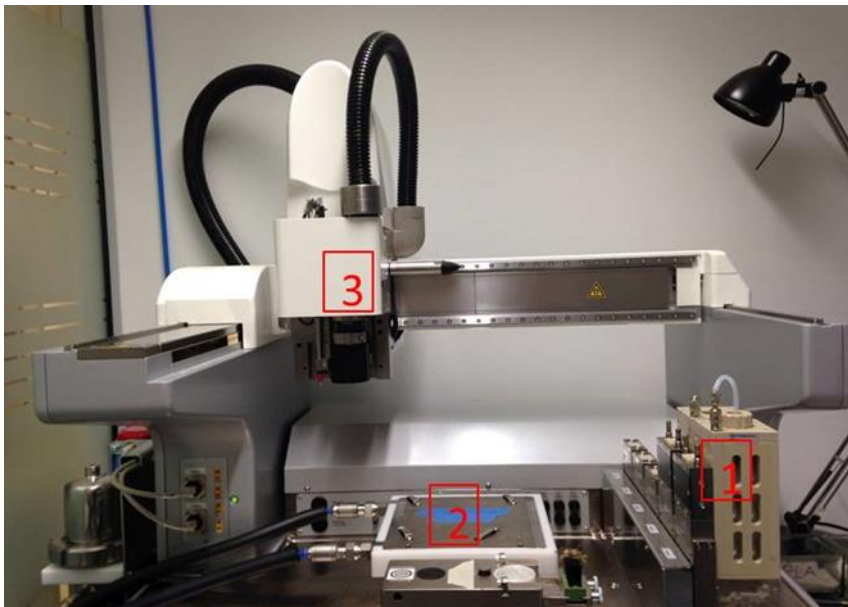


Figure 6. The 3D Bio-plotter system: (1) high temperature cartridge loaded on the pocket; (2) printing plate, equipped with a cooling pad; (3) the robot arm installed with a height sensor (red dot) and a camera.

3.1.4. Sterilization

Cleaning of the scaffold was accomplished by using 75% ethanol alcohol for 15 minutes and keeping them dry overnight in a clean cabinet (hood) under UV light until further analysis was performed.

3.2. Characterization of scaffold

3.2.1. X-ray micro-computed tomography

For quantitative evaluation of surface area and porosity of the scaffolds, μ -CT scans were performed using the SkyScan1172^{VR} microfocus X-ray system (SkyScan^{VR}, Kontich, Belgium) with the CTAn 1.8^{VR} and NRECON RECONSTRUCTIONVR CT software (SkyScan^{VR}). No filter was used to generate the images. Source voltage and current were set at 40 kV and 250 μ A, respectively. After operating CTAn 1.8^{VR} to each reconstructed BMP files, surface area, total porosity percentage and open porosity percentage values were obtained.

3.2.2. Protein adsorption

The 3D printed scaffolds (n=3/group) were placed in 48-well culture plates and rinsed three times with phosphate-buffered saline solution (PBS). Then 1 ml minimum essential medium, alpha modification (α -MEM Gibco Grand Island, NY, USA) supplement with 1% antibiotics (penicillin/ streptomycin, Gibco) and containing 10% fetal bovine serum (FBS, Gibco) was added to each well. After incubating at 37 °C for 2 h, the scaffolds were rinsed with 1 ml PBS for three times to remove the loosely adsorbed proteins. The scaffolds were then transferred to another 48-well plate and incubated with 500 μ l of PBS containing 2.0 wt. % sodium dodecyl sulfate (SDS) for 20 h to remove proteins adsorbed on the scaffold surface. The total protein concentration values in the solutions were quantified by means of a commercial protein assay

kit (BCA; Pierce, Rockford, IL, USA) following the manufacturer's instructions and a microplate reader (FLUOstar optima, BMG LABTECH, Germany) at 530 nm of absorbance.

3.3. Cell cultures and scaffold seeding

To study the cellular reaction on each scaffold surface, HOBs and the mouse fibroblast cell line L929 (American Type Culture Collection CCL 1, Manassas, VA, USA) were used. HOBs were obtained from fresh human mandibular bone specimens, with no clinical or radiographic evidence of pathology, obtained from patients undergoing routine oral surgery at the Department of Maxillofacial Surgery, Haukeland University Hospital and Department of Clinical Dentistry, Faculty of Medicine and Dentistry, University of Bergen, Bergen, Norway. The study protocol for the use of HOBs was approved by The Regional Committees for Medical and Health Research Ethics (REK), Western Norway (2609/610).

The tissue sample was taken from the molar region, washed with (PBS) and digested using collagenase (1mg/mL) in serum-free culture medium using a modification of the method described by Beresford (59). The cells were then characterized using different assays (49).

HOBs were cultured in α -MEM supplement with 1% antibiotics and 10% FBS and incubated at 37°C, 5% CO₂, 95 % humidity until 80% confluence was reached. Three donors with cells from passages 2-5 were used for all studies. Culture medium was changed twice a week. Proliferation of HOBs at 24 hours up to 14 days is shown in Fig.7. Cells were trypsinized and counted using a CountessTM Automated Cell Counter (InvitrogenTM, Carlsbad, CA, USA) then prepared for further experiments. Two variations of 90°/45° pattern 3D printed scaffolds with different distances between the printed fibers (1000 μ m, 1200 μ m) were tested. Scaffolds were soaking for 24 hours in α -MEM supplemented with 1% antibiotics and 10% FBS, then incubated in 5% CO₂ at 37°C. Thereafter, HOBs were seeded onto the various poly (L-lactide-co-caprolactone) scaffolds (shown in **Fig.7**) at a concentration of

1×10^5 cells/scaffold for use in the cell proliferation (MTT) assay and 2×10^5 cells/scaffold for SEM, RNA, L&D, and LDH assays in 48-well plate (Thermo Scientific – nunc, Denmark) for 1, 3, 7, and 14 days. Culture medium was changed twice a week.

The mouse fibroblast cell line L929 was used to optimize scaffold design for proliferation of cells on the 90° or 45° scaffolds. L929 cells were cultured in Dulbecco's modified Eagle's medium (DMEM, Gibco) containing 2 mM L-glutamine (PPA Laboratories GmbH, Pasching, Austria) supplemented with 10% (FBS) and 1% antibiotics at 37°C in a humid atmosphere containing 5% CO_2 for 1, 3 and 7 days.

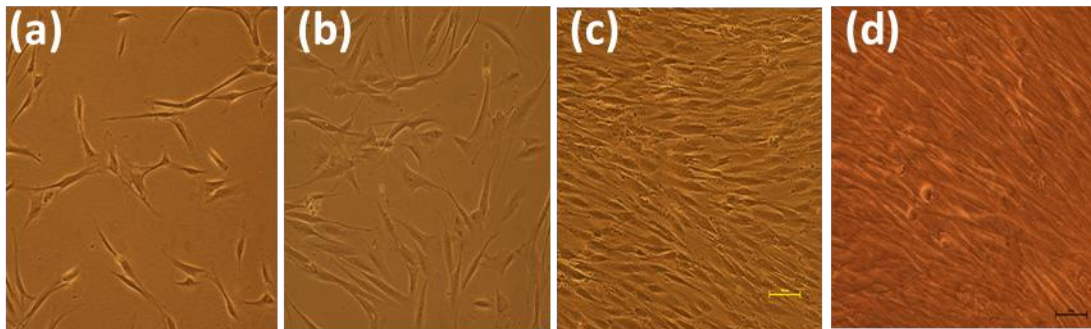


Figure 7. Proliferation of human osteoblasts showing the number of cells after (a) 24 hrs; (b) 3 days; (c) 7 days; (d) 14 days, when the cells reached 80% confluence.

3.3.1. Scanning electron microscopy (SEM)

The HOBs/ scaffolds were fixed in 3% glutaraldehyde for 30 minutes, then washed in 0.1 M Na-cacodylate buffer PH 7.4 for 10 min. The samples were then fixed in 1% osmium tetroxide (OsO_4) in 0.1 M Na-cacodylate buffer without sucrose for 60 min, followed by washing in buffer without sucrose for 2×5 minutes, then washed with distilled water for 5 min and dehydrated in graded ethanol. Critical point drying was carried out and the samples were coated with a 10 nm conducting layer of gold/platinum. The topography of the scaffolds'

surface and cellular morphology were examined in a Jeol JSM (JSM -7400F, Tokyo, Japan) operating at a voltage of 10 kV.

3.3.2. Live and Dead assay (L&D)

cells viability and cytotoxicity were examined using Live/Dead[®] Viability/Cytotoxicity Kit (molecular probes by life technology, North America, USA) and 2×10^5 cells/scaffold grown in a 48-well plate and incubated in 5% CO₂ at 37°C for 1, 3, and 7 days. Culture medium (α -MEM, Gibo) was changed twice a week. For L&D assay the culture medium was replaced with 600 μ l per well from a mixture of (10 ml BPS + 2 μ l calcein AM (white color for detection live cells) + 4 μ l ethidium homodimer-1 (red color for detection dead cells). Cultures were incubated for 35 min and evaluated by fluorescence microscopy (Nikon Eclipse 80i, equipped with 4x, 10x and 20x, Japan).

3.3.3. Lactate dehydrogenase assay (LDH)

Cellular death was also evaluated by measuring the release of LDH from the cells after culture days 1, 3, 7 and 14. The HOB cells were seeded onto scaffolds and placed in 48-well cell culture plates (2×10^5 cells/scaffold) in α -MEM medium, and at each time point the medium was discarded and the cells/scaffolds constructs were washed twice with PBS. Attached cells were lysed with 1% Triton X-100 in PBS for 50 minutes on ice. The released LDH in the cell lysate was measured with a colorimetric LDH detection kit (Abcam, ab102526, Cambridge, UK) according to the manufacturer's instructions. After incubation for 30 min at 37°C the absorbance was measured at 450nm.

3.3.4. Methylthiazol tetrazolium (MTT) assay

The MTT mitochondrial reaction was used to analyze cell proliferation and viability. This is a tetrazolium-based colorimetric assay based on the ability of living cells to reduce yellow tetrazolium dye (Sigma, St Louis, MO, USA) to a purple colored formazan compound (60). HOBs were seeded onto scaffolds at 1×10^5 cells/scaffold and incubated for 1, 3 and 7 days. Cells/scaffold constructs were washed with PBS then 500 μ l MTT reagents (2ml stock of MTT+ 4ml of complete medium) was added to each sample and incubated for 3 hours at 37°C, under a CO₂ (5%) atmosphere. The MTT reagent was removed and cells/scaffold constructs were fixed with Tris-formaline for 5 minutes, washed with distal water and air dried, covered with foil and kept for one day in a dark place. The formazan product was solubilized in 0.5 ml DMSO containing 6.25% (v/v) 0.1 M NaOH 500 μ l for each well by shaking on vibrator for 20 minutes. The end product was quantified by microplate spectrophotometry (BMG LABTECH, GmbH, Germany) at a wavelength of 570 nm and expressed as optical density (OD) units after blank subtraction.

3.4. QRT-PCR gene expression

HOBs were seeded onto scaffolds, placed in 48-well plate with α -MEM culture medium, and allowed to incubate in 5% CO₂ at 37°C for 1, 3, 7, and 14 days for apoptosis assay and 14 days for ALP and OC assay. Culture medium was changed twice a week. At each time point, cells/scaffold were washed with PBS twice and kept in -80°C for further analyses. Total RNA was isolated (from four independent biological replicas) at different culture times using Maxwell® 16 LEV simply RNA Tissue Kit protocol (Promega, Madison, USA), following the manufacturer's instructions. The quantity and quality of the extracted RNA were checked by spectrophotometry. A reverse transcription reaction was performed using the High-Capacity cDNA Archive Kit (Applied Biosystems, Foster City, CA, USA), using 300 ng of

the total RNA dissolved in 40µl nuclease-free water mixed with reverse transcriptase (RT) buffer, random primers, dNTPs and MultiScribe™ RT(ThermoFisher).

Quantitative real-time PCR assays were performed with the ABI StepOnePlus™ RealTime PCR System (Applied Biosystems, Foster City, USA). In each of the RNA samples the GAPDH: Hs99999905_m1 (Applied Biosystems, ThermoFisher Scientific) was used as a reference housekeeping gene. PCR amplification of the selected markers was done in duplicate with 10 µl reaction volume PCR reactions contained 0.5 µl of TaqMan™ (ThermoFisher Scientific) for apoptotic and bone markers (Bax: Hs00180269_m1, Bcl2: Hs00153350_m1, ALP: Hs01029142_m1 and OC: Hs00609452_g1), 3.5 µl of nuclease free water, 5 µl of TaqMan universal fast PCR master mix (Applied Biosystems, ThermoFisher Scientific) and 1 µl cDNA. Thermocycling conditions were 95 °C for 20 s, followed by 40 cycles at 95 °C for 1 s and 60°C for 20 s. The comparative $2^{-\Delta\Delta Ct}$ method (61) was used to calculate the gene expression levels of Bax, Bcl2, ALP and OC in each sample.

3.5. Statistical Analysis

Statistical analysis was performed using IBM SPSS Statistics version 23 (IBM Corp, Armonk, NY,USA) software and One Way Analysis of Variance (ANOVA) was performed at different time points (Multiple Comparison tests, followed by Tukey Test). The Differences between the means were considered statistically significant at $P<0.05$. Student T-test was performed to check the differences in means between the scaffolds for LDH and µ CT test, statistical significance was considered at $P<0.05$.

4. Results

4.1. Scaffold fabrication:

Two different scaffold designs were produced with a layer rotation of 45° and 90° and a distance of 1000 μm and 1200 μm between the printed fibers as shown in **Fig.8**.

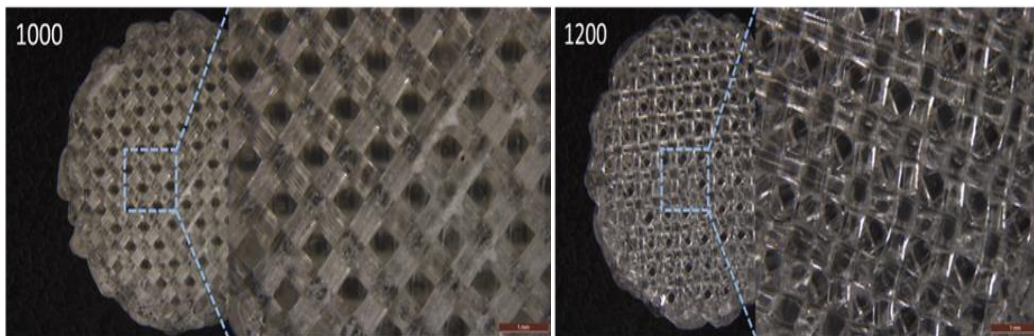


Figure 8. The pores of the two modified patterns of 3D printed scaffolds (1000 μm and 1200 μm) are shown using the LEICA M205C microscopy.

4.2. Characterization of scaffolds

4.2.1. Microcomputed tomography analysis (μCT)

The interconnected pore structure of the scaffolds was analyzed by μCT , the total porosity (%), open porosity (%), and surface area (mm^2) are shown in **Table 1 and 2** and **Fig. 9, 10, 11** and **12**. There was no statistically significant difference between the two designs, although the 1200 μm scaffold showed higher porosity than the 1000 μm scaffold.

Table 1. μ CT analysis of the 1200 μ m 3D printed scaffold.

1200	Sample 1	Sample 2	Sample 3	Average	SD
Total volume (mm ³)	135	115	137	129	12,16553
Object volume (mm ³)	67,9	48	63,8	59,9	10,50762
Percent object volume	50,2	41,6	46,5	46,1	4,313931
Object surface (mm ²)	634,7	519,8	611,8	588,7667	60,8145
Closed porosity (%)	0,14	0,14	0,04	0,106667	0,057735
Open porosity (%)	49,6	58,2	53,4	53,733333	4,309679

Table 2. μ CT analysis of the 1000 μ m 3D printed scaffold.

1000	Sample 1	Sample 2	Sample 3	Average	SD
Total volume (mm ³)	114,6	172,3	184,2	157,0333	37,22692
Object volume (mm ³)	68,4	125,8	121,4	105,2	31,94558
Percent object volume	59,6	73	65,9	66,16667	6,703979
Object surface (mm ²)	646,9	741	792,8	726,9	73,96492
Closed porosity (%)	0,2	0,3	0,2	0,233333	0,057735
Open porosity (%)	40,1	26,7	33,9	33,56667	6,706216

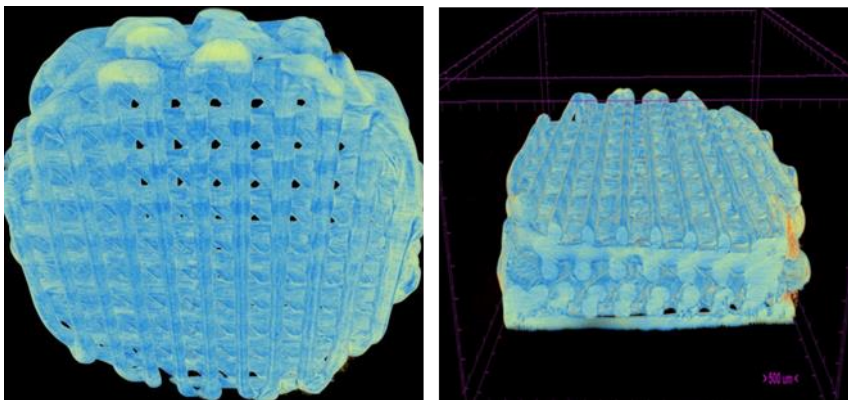


Figure 9. Reconstructed μ CT figure confirming the open, porous structure of the printed scaffolds.

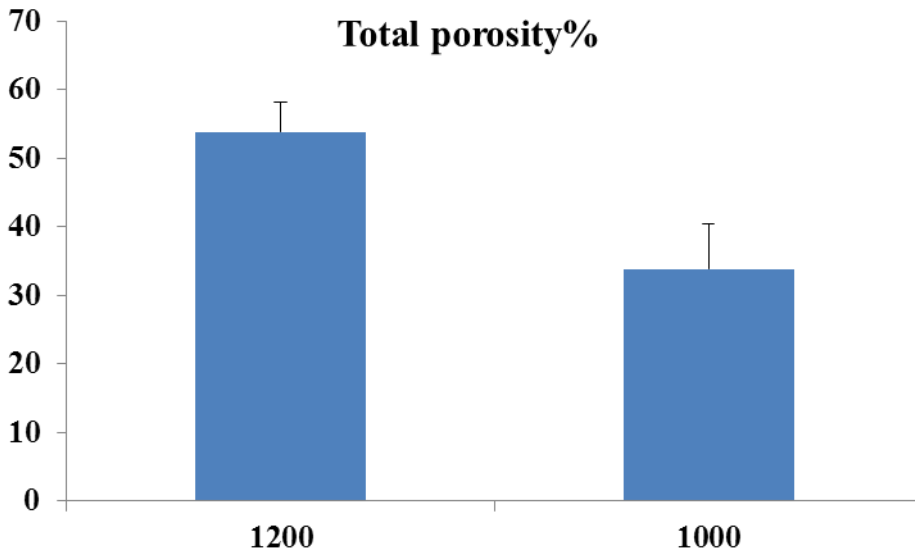


Figure 10. μ CT analysis of total porosity% for two scaffold designs

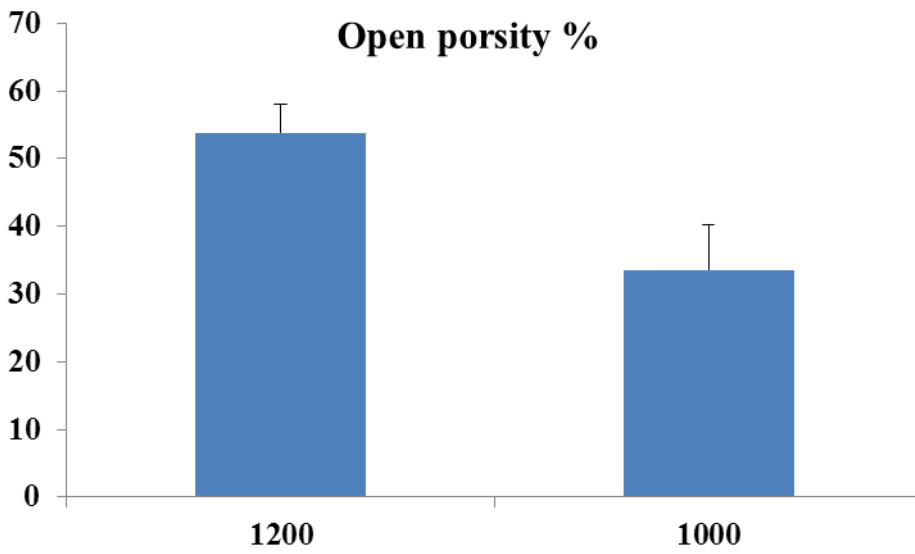


Figure 11. μ CT analysis of open porosity % for two scaffold designs

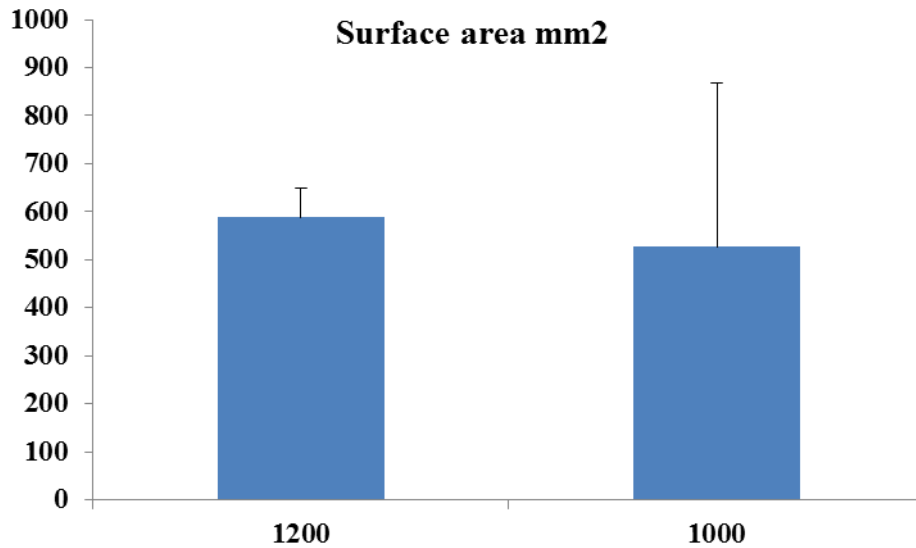


Figure 12. μ CT analysis of surface area mm² for two scaffold designs

4.2.2. Protein adsorption

After two h incubation, the total protein concentration in the solutions on modified 90°/45° patterns (1000 μ m, 1200 μ m) was determined. The results showed only a slight difference in the total protein concentration values of the solutions from the modified 90°/45° pattern (1000 μ m, 1200 μ m) 3D printed scaffolds (**Fig.13**). Although the scaffold with 1200 μ m distance between the fibers demonstrated more protein adsorption than the 1000 μ m scaffolds, it was not statistically significant.

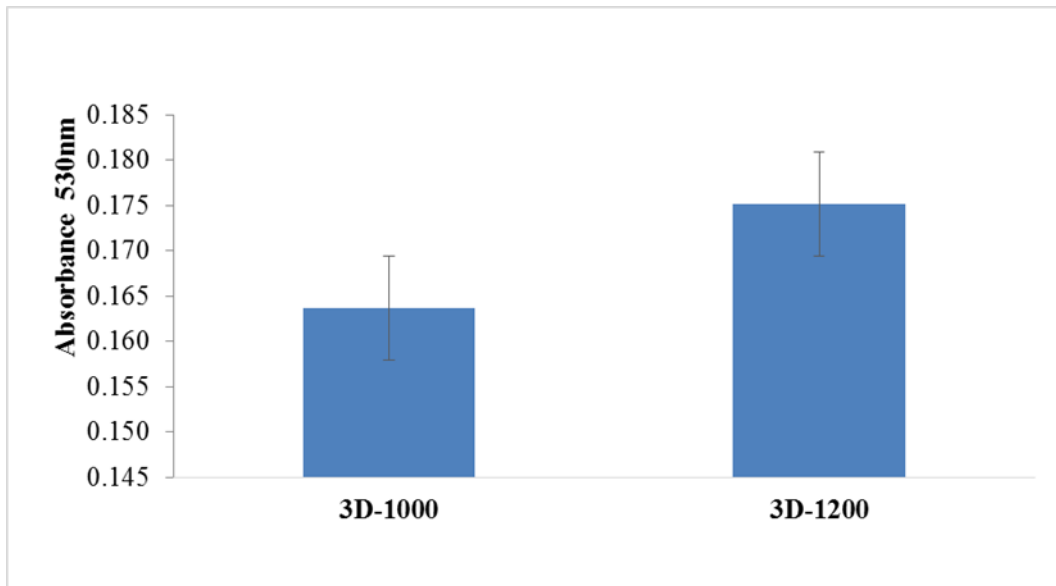


Figure 13. Protein adsorption on the surface of the two printed scaffolds

4.3. Cellular activities

4.3.1. Cell proliferation

L929 mouse fibroblast cells were seeded and cultured on (0/90° and 0/45°) 3D printed scaffolds for 1, 3 and 7 days for optimization of the proliferation of cells on the scaffolds. The MTT results showed an increase in the proliferation of cells from day 1 to day 7 on scaffolds compared to the 2D control (48 well-plates) (**Fig.14** and **15**). Higher MTT activity was shown on the 3D printed scaffolds than on the 2D tissue culture plastic ($P < 0.05$).

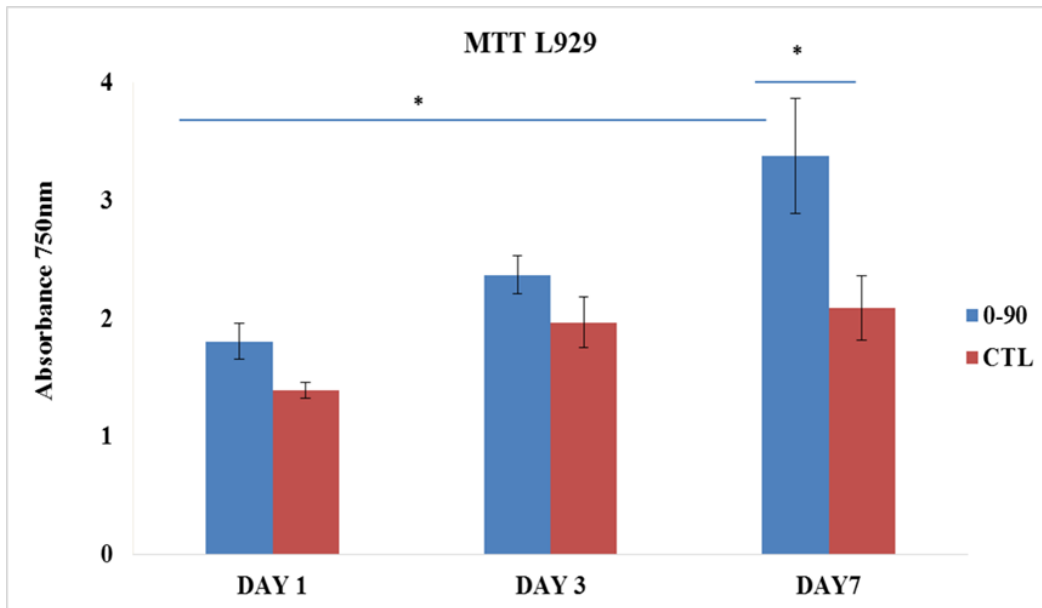


Figure 14. MTT assay. L929 mouse fibroblast cells seeded on 3D printed scaffold with struts angle 0-90°

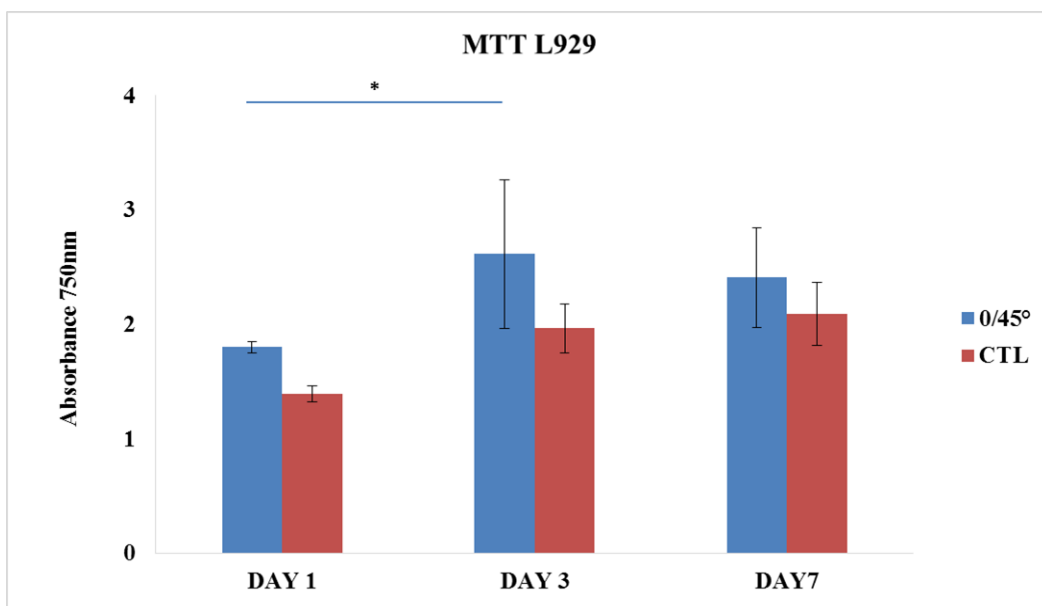


Figure 15. MTT assay. L929 mouse fibroblast cells seeded on 3D printed scaffold with struts angle 0-45°

4.3.2. Cell morphology and cell attachment

SEM images of cell morphology showed that after incubation for 1 day HOBs were attached to the inner layers of the two modified designs and had normal osteoblast morphology. After incubation for 3 days the HOBs were evenly distributed on the surfaces of the two scaffolds and cells had migrated to the middle of the scaffolds. After incubation for 7 and 14 days HOBs were confluent on the two scaffolds' surfaces (Fig.16).

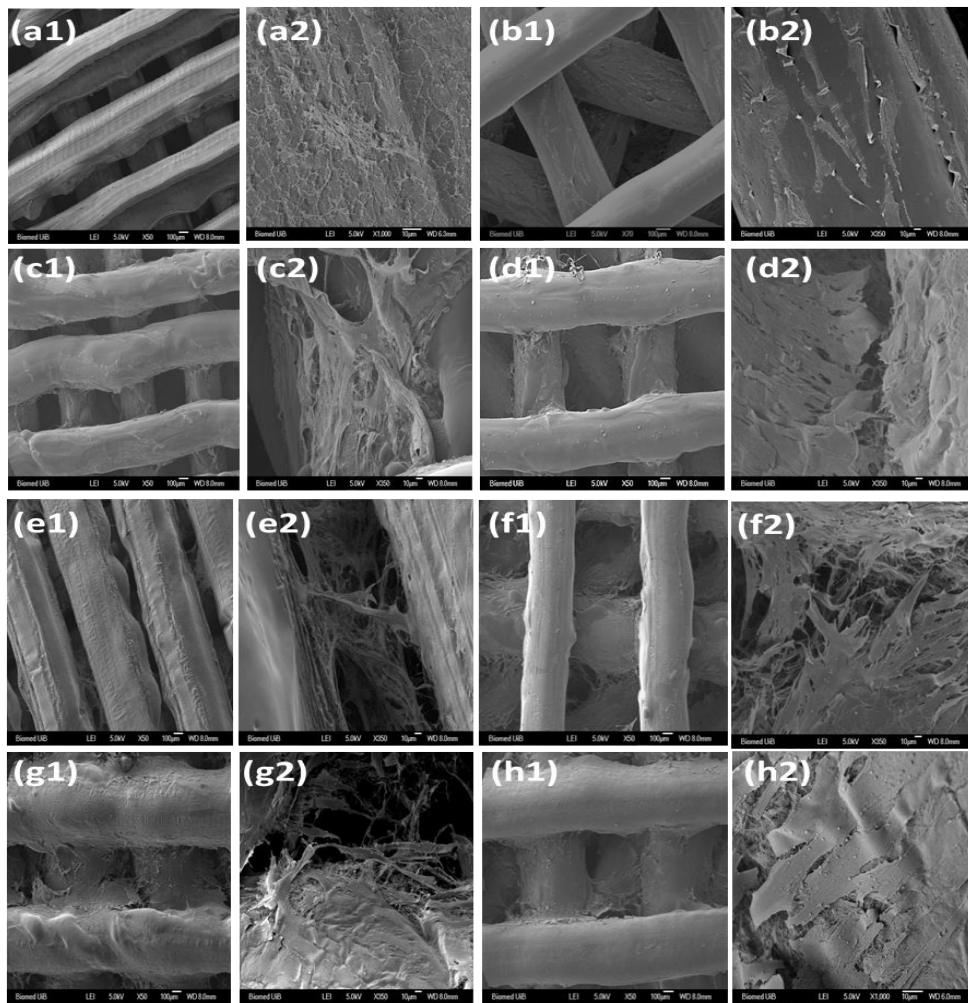


Figure 16. SEM images of scaffolds cultured with HOBs. Magnification 50× of 1000 μm (a1, c1, e1, g1) and 1200 μm (b1, d1, f1, h1) 3D-printed scaffold cultured for 1, 3, 7, and 14 days respectively. Magnification 350× of 1000 μm (a2, c2, e2, g2) and 1200 μm (b2, d2, f2, h2) 3D-printed scaffold cultured for 1, 3, 7, and 14 days respectively.

4.3.3. Cell viability Live / dead assay

The L&D assay carried out using calcein/ethidium staining after seven days of culture (**Fig.17**), showed most of the cells exhibiting green rather than red fluorescence, indicating cell viability. Cells showed normal osteoblast morphology on both scaffolds.

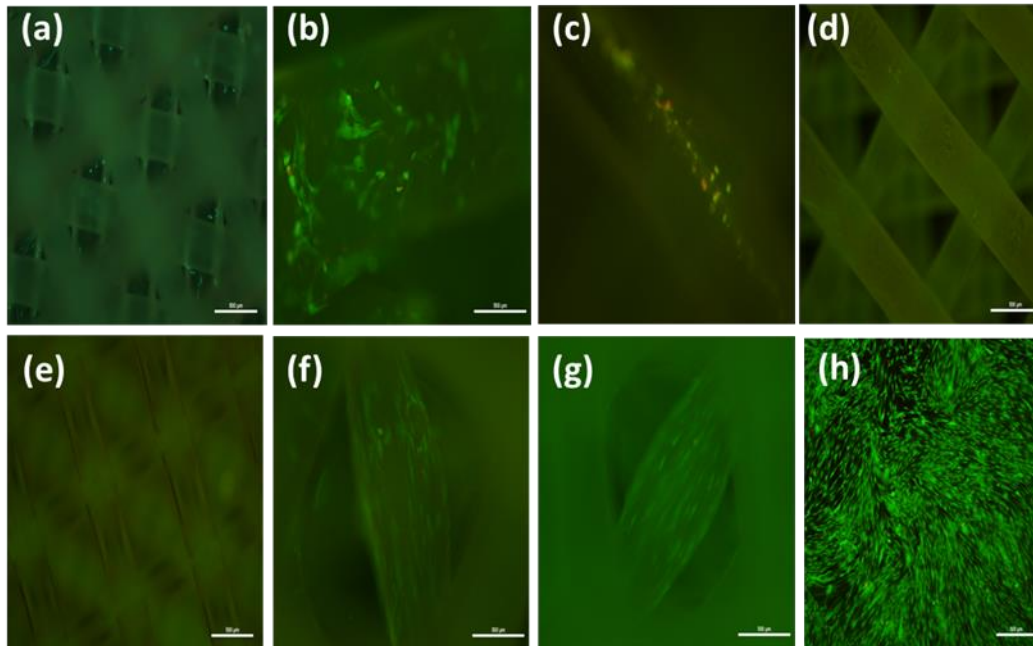


Figure 17. Fluorescence microscopy images of human osteoblast cells after staining with fluorescein (green-live cells) calcein AM and ethidium homodimer-1 (red-dead cells). (a,b) HOB proliferation in 3DP scaffold 1000 day 1, (c,d) 1200 day 3, (e) 1000 day 3, (f) 1000 day 7, (g) 1200 day 7, (h) HOB in control day 7.

4.3.4. LDH assay

The cytotoxicity of 3D printed scaffolds evaluated by the LDH assay showed HOBs were able to grow and proliferate well (**Fig.18**). Statistically there was no significance difference between the two designs.

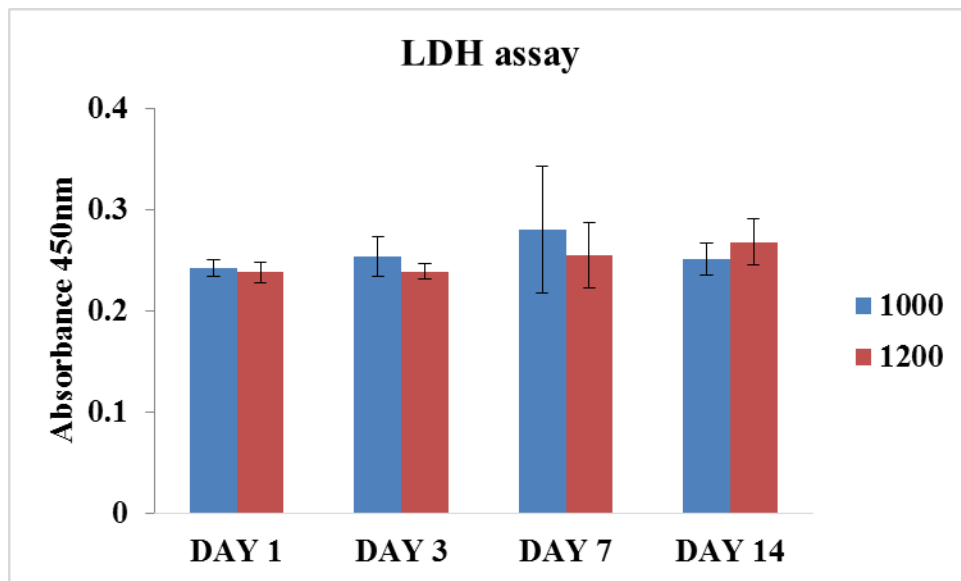


Figure 18. LDH cytotoxicity assay.

4.3.5. MTT assay

As shown in **Fig. 19**, the MTT assay indicated that the 3D printed scaffolds enhanced cell proliferation, with no significant difference between 1200 and 1000 3D printed scaffolds.

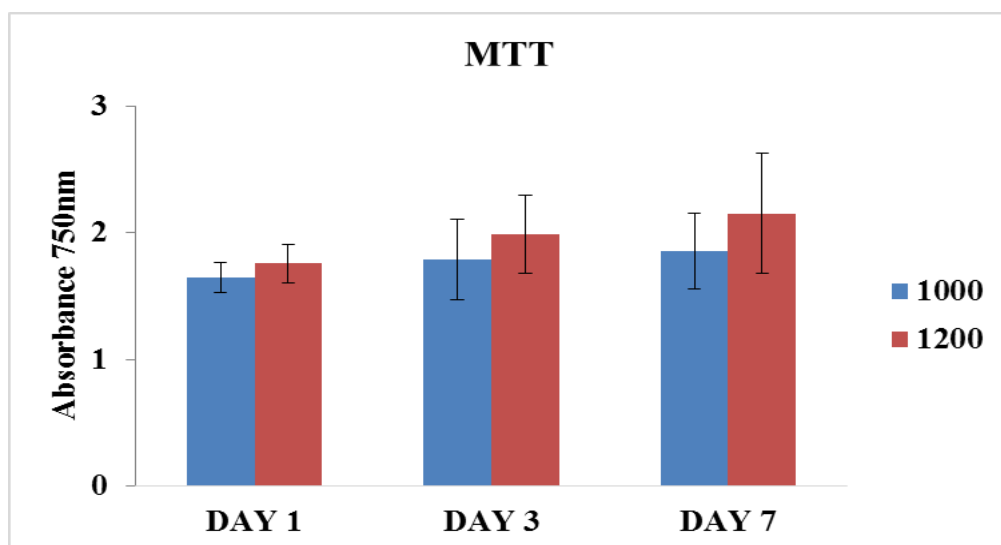


Figure 19. MTT assay for cell proliferation.

4.4. qRT-PCR

4.4.1. Apoptosis

The results for the cell death assay (**Fig. 20**) demonstrated no statistical significant difference between the mRNA expression of Bax by HOBs seeded onto 1000 μm and 1200 μm fiber separation scaffolds at days 1,3, 7 and 14 ($P>0.05$). However, significant differences were observed between mRNA expression of Bcl2 by HOBs seeded onto 1000 μm and 1200 μm scaffolds at days 1, 3, 7 and 14 ($P<0.05$). At all these time-points, better cell viability and decreased cell death was seen with the 1200 μm scaffolds.

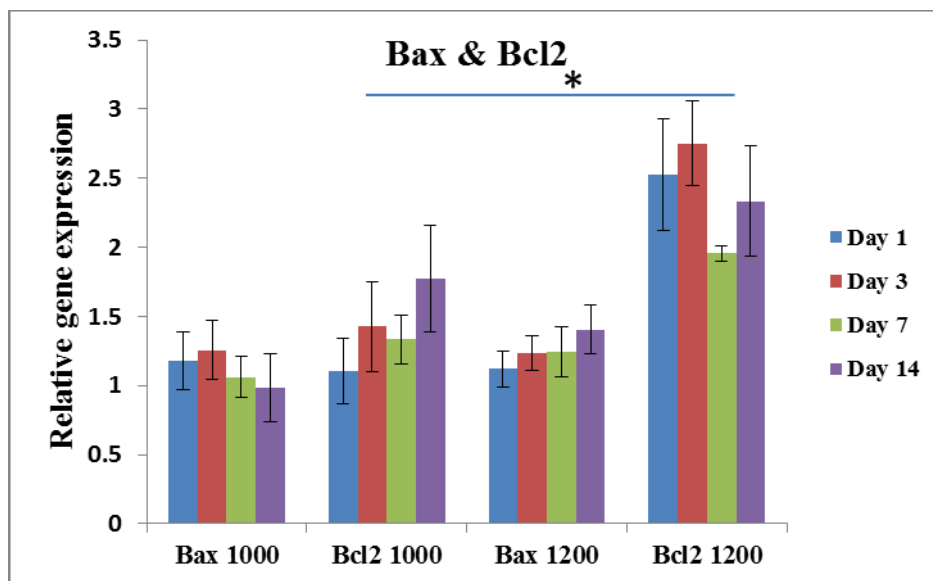


Figure 20. Gene expressions of Bax and Bcl2 from HOBs seeded on 3D printed scaffolds (1000 and 1200 μm)

4.4.2. Bone markers

To evaluate osteogenic differentiation on the two scaffolds, the mRNA expression of ALP and OC were determined at day 14 using probes specific for each gene normalized to the housekeeping gene GAPDH. ALP and OC expression from cells on the 1200 μm scaffolds at

day 14 were higher than on the 1000 μm scaffolds, although there was no significant difference found at day 14 between mRNA levels of ALP of HOBs seeded onto 1000 μm and 1200 μm scaffolds. On the other hand, there was a statistically significant difference between mRNA levels of OC of HOBs seeded onto 1000 μm and 1200 μm at day 14 ($P < 0.05$) (Fig. 21).

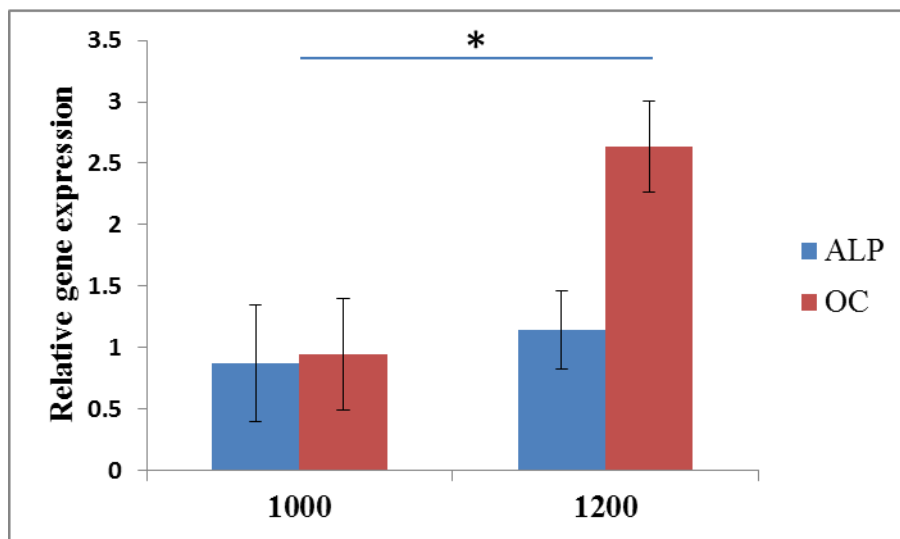


Figure 21. ALP and OC expression from HOBs seeded on 3D printed scaffolds (1000 μm and 1200 μm).

5. Discussion

Recently, 3D printing has emerged in the tissue engineering field as a new tool for the fabrication of scaffolds to produce well-defined and reproducible architectures. 3D printing allows the building of custom-made scaffolds based on patient-specific tissue defects. These 3D printed scaffolds also provide good *in vitro* platforms for studying the effects of geometry/architecture on cellular responses, hopefully leading to improved mechanical performance of bioengineered scaffolds. The “printing” process involves many interactions between hardware, software and material properties. Therefore, choosing the right processing conditions and the proper materials helps in obtaining reproducible and high quality 3D scaffolds. Several degradable polymers such as polycaprolactone, polylactic acid (PLA), polyglycolic acid, and their copolymers have been used to fabricate 3D printed scaffolds (62, 63). The advantages of using a synthetic polymer and their copolymer materials are ease in processing into tissue engineering scaffolds and extreme versatility, which allow custom tailoring, and the ability to vary biodegradation time, softness, wettability, mechanical strength, and biocompatibility (3, 32). These synthetic polymers have also been approved by the US FDA for clinical use, so that PLCL is already in use as a biodegradable polymer for tissue engineering applications. Though this polymer has been extensively used to fabricate a 3D porous scaffold using the salt-leaching method, the use of the 3D printing technique using a nozzle based system has rarely been reported (62). In the present study, 3D scaffolds were plotted layer-by-layer with different angles of layer rotation and distances between the printed struts. The fiber spacing was fixed at 1mm and 1.2 mm, respectively as shown in Fig. 5. Angles of 45° (0/45) and 90° (0/90) rotations were applied between each pair of continuous layers (Fig. 4). The angle of 0/45 yielded scaffolds with rhomboid pores while the angle of 0/90 produced a scaffold with square pores. The design of these scaffolds was chosen to make each layer act as a barrier to the next layer when cell solution flows, to increase the

possibility of cell attachment (46). The selected design and material allowed well-defined porous scaffolds to be obtained, as observed by light microscope (Fig. 8) and μ CT (Fig. 9). It is well known that a scaffold with open porous interconnectivity is a crucial factor for tissue engineering applications. Connected pores allow the diffusion of nutrients and cell metabolite and improve cellular proliferation and migration (46, 64). Theoretically, the bigger the distance between the printed struts, the more open porosity that is obtained. The results obtained from μ Ct analysis showed that the design with a distance of 1200 μ m between fibers had more open porosity when compared to 1000 μ m. During the printing process, it is possible that some fusion between the struts and the underlying layers occurred with the smaller distance between fibers, perhaps explaining why μ CT evaluations of porosity of the 1000 μ m design were lower than the 1200 μ m.

A biocompatible scaffold with appropriate surface properties such as surface area and wettability is important for protein adsorption, which is a crucial step in the bone regeneration process. The first event that takes place when a scaffold is implanted *in vivo*, after the initial hydration, is protein adsorption on the surface. This step drives subsequent cell adhesion, followed by proliferation and/or differentiation (65). Li et al. (66) showed that high specific surface area scaffold architecture can increase protein adsorption. In this study, however, we found no significant difference in protein adsorption on the surface of the printed scaffolds between the two designs. This result is in agreement with the results of surface area obtained from μ CT analysis (Tables 1 and 2).

The cytotoxicity and biocompatibility of scaffolds made of poly (L-lactide-co-caprolactone) have previously been evaluated by culturing L929 mouse cells and HOBs (35), and cell proliferation and expression of apoptotic markers were consistent with good biocompatibility of the scaffolds. In the present study, the 3D printed scaffolds again demonstrated good biocompatibility and provided greater surface area for cell growth than the

2D tissue culture plates. The MTT assay of cultured HOBs on the modified scaffolds showed no significant difference between the 1000 and 1200 μm versions. This could be due to the comparable surface area of the two designs as shown in the μCT study (Fig. 12).

SEM analysis shows that HOB cells responded well to the two versions of the 3D printed scaffolds, with good attachment, proliferation (day 1 to 7), even distribution and formation of multicellular layers (day 14) which entirely covered the scaffolds (Fig. 16). A previous study performed by our group on the same scaffold design compared the 3D printed scaffolds with salt leached scaffolds, and showed that the homogeneous cell distribution on 3D printed scaffolds provides improved nutrition that facilitates the spreading and proliferation of the HOBs relative to that seen on the salt-leached scaffolds (36, 41, 46).

The viability of cells on the 3D printed scaffolds was investigated using the Live/Dead[®] Viability/Cytotoxicity Kit. The fluorescence microscopy images of the 3D printed scaffolds at 7d after being seeded with HOBs is shown in Fig.17 (live cells are green and red cells are dead). This type of assay allows the detection HOBs on the 3D printed scaffolds, and, in agreement with the previous study by Oliveira et al (67) demonstrated adhesion, proliferation and viability after 7 days in culture with no significant difference between the two versions of the scaffolds. Furthermore, it can be seen that HOBs penetrated deep in between the layers of the two modified designs of the 3D printed scaffold.

The LDH assay was used to detect cell death by measuring the release of LDH from the cells when the cell membrane of the HOBs was damaged. The LDH assay was used as another measure of cell viability and proliferation at different time points. No statistically significant differences were seen for the two versions of the 3D printed scaffolds (Fig.18), in agreement with a previous study (68). The results demonstrated the biocompatibility of the two types of scaffolds *in vitro*, promoting HOB proliferation without cytotoxic effect (35).

Enhanced growth of HOBs on the two versions of the 3D printed scaffolds was seen and clearly demonstrated by the MTT assay (Fig. 19). Cell growth and proliferation on the 1200 μm 3D printed scaffolds was better than on the 1000 μm 3D printed scaffold. MTT analysis disclosed that HOBs had responded well to both the 1000 μm and 1200 μm PLCL scaffolds, and there was a continual increase of cells on 3D printed scaffolds up to day 7 with no statistically significant difference between the two designs. These results are in agreement with a previous study by Sun et al (46) in that their 3D printed scaffolds, made from biodegradable poly (L-lactide-co-caprolactone), were also biocompatible with HOB cells, did not inhibit attachment and allowed proliferation of cells.

Apoptosis, or programmed cell death, involves both Bcl2 (an anti-apoptotic gene) and Bax (a pro-apoptotic gene) (28, 69). Apoptotic activity in HOBs on the 3D printed scaffolds was examined by quantitative real time RT-PCR. Our results showed that the mRNA expression level of Bcl2 measured by qRT-PCR on days 1, 3, 7 and 14 increased, while mRNA expression level of Bax decreased in both scaffold version, indicating that the apoptotic activity did not increase in the cells seeded onto the modified 3D printed scaffolds i.e. there was continuous increase in cell viability and decrease in cell death. Moreover, the mRNA expression level of Bcl2 was higher in cells seeded onto the 1200 μm scaffold compared to 1000 μm . Our data is in agreement with a previous study that showed similar reduction of apoptotic activity when the same cells were seeded on similar copolymer material scaffolds (35).

To further evaluate the *in vitro* osteogenic potential of the two versions of the 3D printed scaffolds, the bone markers ALP and OC were tested at day 14 using qRT-PCR. The results showed higher expression of mRNA of ALP and OC by HOBs grown on the 1200 μm than by HOBs grown on the 1000 μm 3D printed scaffolds. ALP is considered an early marker of osteoblast differentiation (19), and OC a late marker of bone formation, or a mature

differentiation marker, in HOBs (19). The modified 3D printed scaffolds supported better expression of the early and late osteoblast markers ALP and OC, respectively, possibly because of the modified design that stimulated osteogenic differentiation. Falguni et al (70) reported an increase in ALP and OC by human inferior turbinate nasal tissue-derived mesenchymal stromal cells cultured on cell-laid mineralized extracellular matrix-ornamented 3D scaffolds at day 7 and 14.

The presented study showed that the two 3D printed copolymer scaffolds versions (1000 μm and 1200 μm) are biocompatible with HOBs, and do not impair cell attachment or proliferation. Cell viability and apoptosis assays reflected good cell growth and proliferation. Enhanced osteoblast proliferation and differentiation were demonstrated by increased mRNA expression of ALP and OC. Therefore, the HOBs/1200 μm scaffolds warrant further investigation *in vivo* as promising constructs for application in bone tissue engineering.

6. Conclusions

PLCL scaffolds were successfully produced with a 3D printer and the two different designs investigated in this study demonstrated comparable porosity and surface area. The HOB cells attached, spread and proliferated well onto the 3D printed PLCL scaffolds. Cell viability and apoptosis assays demonstrated good cell growth and proliferation. Osteoblast proliferation and differentiation were demonstrated by increased mRNA expression of the ALP and OC genes. Compared to the 1000 μ m scaffold, the 1200 μ m scaffold supported better osteoblast maturation and increased the secretion of bone matrix, which aids in bone engineering. Further *in vivo* studies are therefore warranted.

7. References

1. Langer R, Vacanti JP. Tissue engineering. *Science*. 1993;260(5110):920-6.
2. Rose FRAJ, Oreffo ROC. Bone Tissue Engineering: Hope vs Hype. *Biochemical and Biophysical Research Communications*. 2002;292(1):1-7.
3. Chan BP, Leong KW. Scaffolding in tissue engineering: general approaches and tissue-specific considerations. *European Spine Journal*. 2008;17(4):467-79.
4. Nukavarapu SP, Dorcenus DL. Osteochondral tissue engineering: current strategies and challenges. *Biotechnol Adv*. 2013;31(5):706-21.
5. O'Keefe RJ, Mao J. Bone tissue engineering and regeneration: from discovery to the clinic--an overview. *Tissue Eng Part B Rev*. 2011;17(6):389-92.
6. Cowan CM, Soo C, Ting K, Wu B. Evolving Concepts in Bone Tissue Engineering. *Current Topics in Developmental Biology*. Volume 66: Academic Press; 2005. p. 239-85.
7. Amini AR, Laurencin CT, Nukavarapu SP. Bone tissue engineering: recent advances and challenges. *Crit Rev Biomed Eng*. 2012;40(5):363-408.
8. Turhani D, Weissenbock M, Stein E, Wanschitz F, Ewers R. Exogenous recombinant human BMP-2 has little initial effects on human osteoblastic cells cultured on collagen type I coated/noncoated hydroxyapatite ceramic granules. *J Oral Maxillofac Surg*. 2007;65(3):485-93.
9. Oryan A, Alidadi S, Moshiri A, Maffulli N. Bone regenerative medicine: classic options, novel strategies, and future directions. *J Orthop Surg Res*. 2014;9(1):18.
10. Herten M, Rothamel D, Schwarz F, Friesen K, Koegler G, Becker J. Surface- and nonsurface-dependent in vitro effects of bone substitutes on cell viability. *Clin Oral Investig*. 2009;13(2):149-55.
11. Zhao S, Zhang J, Zhu M, Zhang Y, Liu Z, Tao C, et al. Three-dimensional printed strontium-containing mesoporous bioactive glass scaffolds for repairing rat critical-sized calvarial defects. *Acta Biomater*. 2015;12:270-80.
12. Baum BJ, Mooney DJ. THE IMPACT OF TISSUE ENGINEERING ON DENTISTRY. *The Journal of the American Dental Association*. 2000;131(3):309-18.
13. Finkemeier CG. Bone-Grafting and Bone-Graft Substitutes. *The Journal of Bone & Joint Surgery*. 2002;84(3):454-64.
14. Lee K, Majumdar MK, Buyaner D, Hendricks JK, Pittenger MF, Mosca JD. Human Mesenchymal Stem Cells Maintain Transgene Expression during Expansion and Differentiation. *Mol Ther*. 2001;3(6):857-66.
15. Blau HM, Brazelton TR, Weimann JM. The evolving concept of a stem cell: entity or function? *Cell*. 2001;105(7):829-41.
16. Seong JM, Kim BC, Park JH, Kwon IK, Mantalaris A, Hwang YS. Stem cells in bone tissue engineering. *Biomed Mater*. 2010;5(6):062001.
17. Grellier M, Bordenave L, Amédée J. Cell-to-cell communication between osteogenic and endothelial lineages: implications for tissue engineering. *Trends in Biotechnology*. 2009;27(10):562-71.
18. Guillot PV, Cui W, Fisk NM, Polak DJ. Stem cell differentiation and expansion for clinical applications of tissue engineering. *J Cell Mol Med*. 2007;11(5):935-44.
19. Aubin JE. Bone stem cells. *Journal of cellular biochemistry Supplement*. 1998;30-31:73-82.
20. Jadlowiec JA, Celil AB, Hollinger JO. Bone tissue engineering: recent advances and promising therapeutic agents. *Expert Opin Biol Ther*. 2003;3(3):409-23.
21. Salgado AJ, Coutinho OP, Reis RL. Bone tissue engineering: state of the art and future trends. *Macromol Biosci*. 2004;4(8):743-65.

22. Seitz H, Rieder W, Irsen S, Leukers B, Tille C. Three-dimensional printing of porous ceramic scaffolds for bone tissue engineering. *Journal of Biomedical Materials Research Part B: Applied Biomaterials*. 2005;74B(2):782-8.
23. Müller B, Deyhle H, Fierz FC, Irsen SH, Yoon JY, Mushkolaj S, et al., editors. *Biomimetic hollow scaffolds for long bone replacement* 2009.
24. Hutmacher DW. Scaffolds in tissue engineering bone and cartilage. *Biomaterials*. 2000;21(24):2529-43.
25. Butscher A, Bohner M, Hofmann S, Gauckler L, Müller R. Structural and material approaches to bone tissue engineering in powder-based three-dimensional printing. *Acta biomaterialia*. 2011;7(3):907-20.
26. Rhodes N. Biocompatibility testing of tissue engineered products. *Vox Sang*. 2004;87 Suppl 2:161-3.
27. Allen M, Millett P, Dawes E, Rushton N. Lactate dehydrogenase activity as a rapid and sensitive test for the quantification of cell numbers in vitro. *Clin Mater*. 1994;16(4):189-94.
28. Adams JM, Cory S. The Bcl-2 protein family: arbiters of cell survival. *Science*. 1998;281(5381):1322-6.
29. Ma PX. Biomimetic materials for tissue engineering. *Adv Drug Deliv Rev*. 2008;60(2):184-98.
30. Mano JF, Sousa RA, Boesel LF, Neves NM, Reis RL. Bioinert, biodegradable and injectable polymeric matrix composites for hard tissue replacement: state of the art and recent developments. *Composites Science and Technology*. 2004;64(6):789-817.
31. Peppas NA, Langer R. New challenges in biomaterials. *Science*. 1994;263(5154):1715-20.
32. Li X, Cui R, Sun L, Aifantis KE, Fan Y, Feng Q, et al. 3D-Printed Biopolymers for Tissue Engineering Application. *International Journal of Polymer Science*. 2014;2014:13.
33. Nair L, Laurencin C. Polymers as Biomaterials for Tissue Engineering and Controlled Drug Delivery. In: Lee K, Kaplan D, editors. *Tissue Engineering I. Advances in Biochemical Engineering/Biotechnology*. 102: Springer Berlin Heidelberg; 2006. p. 47-90.
34. Chen G, Sato T, Ushida T, Hirochika R, Shirasaki Y, Ochiai N, et al. The use of a novel PLGA fiber/collagen composite web as a scaffold for engineering of articular cartilage tissue with adjustable thickness. *J Biomed Mater Res A*. 2003;67(4):1170-80.
35. Idris SB, Dänmark S, Finne-Wistrand A, Arvidson K, Albertsson A-C, Bolstad AI, et al. Biocompatibility of Polyester Scaffolds with Fibroblasts and Osteoblast-like Cells for Bone Tissue Engineering. *Journal of Bioactive and Compatible Polymers*. 2010;25(6):567-83.
36. Idris SB, Arvidson K, Plikk P, Ibrahim S, Finne-Wistrand A, Albertsson AC, et al. Polyester copolymer scaffolds enhance expression of bone markers in osteoblast-like cells. *J Biomed Mater Res A*. 2010;94(2):631-9.
37. Gurav N, Downes S. A qualitative in vitro evaluation of the degradable materials poly(caprolactone), poly(hydroxybutyrate) and a poly(hydroxybutyrate)-(hydroxyvalerate) copolymer. *Journal of Materials Science: Materials in Medicine*. 1994;5(11):784-7.
38. Migliaresi C, Fambri L, Cohn D. A study on the in vitro degradation of poly(lactic acid). *Journal of biomaterials science Polymer edition*. 1994;5(6):591-606.
39. Ulery BD, Nair LS, Laurencin CT. Biomedical Applications of Biodegradable Polymers. *Journal of polymer science Part B, Polymer physics*. 2011;49(12):832-64.
40. Nair LS, Laurencin CT. Biodegradable polymers as biomaterials. *Progress in Polymer Science*. 2007;32(8-9):762-98.
41. Dänmark S, Finne-Wistrand A, Wendel M, Arvidson K, Albertsson A-C, Mustafa K. Osteogenic Differentiation by Rat Bone Marrow Stromal Cells on Customized Biodegradable Polymer Scaffolds. *Journal of Bioactive and Compatible Polymers*. 2010;25(2):207-23.

42. Huang L, Hu J, Lang L, Wang X, Zhang P, Jing X, et al. Synthesis and characterization of electroactive and biodegradable ABA block copolymer of polylactide and aniline pentamer. *Biomaterials*. 2007;28(10):1741-51.
43. Mathieu LM, Montjovent MO, Bourban PE, Pioletti DP, Manson JA. Bioresorbable composites prepared by supercritical fluid foaming. *J Biomed Mater Res A*. 2005;75(1):89-97.
44. Whang K, Thomas CH, Healy KE, Nuber G. A novel method to fabricate bioabsorbable scaffolds. *Polymer*. 1995;36(4):837-42.
45. Bose S, Vahabzadeh S, Bandyopadhyay A. Bone tissue engineering using 3D printing. *Mater Today*. 2013;16.
46. Sun Y, Finne-Wistrand A, Albertsson AC, Xing Z, Mustafa K, Hendrikson WJ, et al. Degradable amorphous scaffolds with enhanced mechanical properties and homogeneous cell distribution produced by a three-dimensional fiber deposition method. *J Biomed Mater Res A*. 2012;100(10):2739-49.
47. Linez-Bataillon P, Monchau F, Bigerelle M, Hildebrand HF. In vitro MC3T3 osteoblast adhesion with respect to surface roughness of Ti6Al4V substrates. *Biomol Eng*. 2002;19(2-6):133-41.
48. Morra M, Cassinelli C, Bruzzone G, Carpi A, Di Santi G, Giardino R, et al. Surface chemistry effects of topographic modification of titanium dental implant surfaces: 1. Surface analysis. *Int J Oral Maxillofac Implants*. 2003;18(1):40-5.
49. Mustafa K, Wroblewski J, Hulthenby K, Lopez BS, Arvidson K. Effects of titanium surfaces blasted with TiO₂ particles on the initial attachment of cells derived from human mandibular bone. A scanning electron microscopic and histomorphometric analysis. *Clin Oral Implants Res*. 2000;11(2):116-28.
50. Hou Q, Grijpma DW, Feijen J. Porous polymeric structures for tissue engineering prepared by a coagulation, compression moulding and salt leaching technique. *Biomaterials*. 2003;24(11):1937-47.
51. Schander K, Arvidson K, Mustafa K, Hellem E, Bolstad AI, Wistrand AF-, et al. Response of Bone and Periodontal Ligament Cells to Biodegradable Polymer Scaffolds In Vitro. *Journal of Bioactive and Compatible Polymers*. 2010.
52. Vandrovcova M, Bacakova L. Adhesion, growth and differentiation of osteoblasts on surface-modified materials developed for bone implants. *Physiol Res*. 2011;60(3):403-17.
53. Serra T, Mateos-Timoneda MA, Planell JA, Navarro M. 3D printed PLA-based scaffolds: a versatile tool in regenerative medicine. *Organogenesis*. 2013;9(4):239-44.
54. Zhu X, Chen J, Scheideler L, Altebaeumer T, Geis-Gerstorfer J, Kern D. Cellular reactions of osteoblasts to micron- and submicron-scale porous structures of titanium surfaces. *Cells Tissues Organs*. 2004;178(1):13-22.
55. Price RL, Ellison K, Haberstroh KM, Webster TJ. Nanometer surface roughness increases select osteoblast adhesion on carbon nanofiber compacts. *J Biomed Mater Res A*. 2004;70(1):129-38.
56. Yilgor P, Sousa RA, Reis RL, Hasirci N, Hasirci V. 3D Plotted PCL Scaffolds for Stem Cell Based Bone Tissue Engineering. *Macromolecular Symposia*. 2008;269(1):92-9.
57. Ruiz-Cantu L, Gleadall A, Faris C, Segal J, Shakesheff K, Yang J. Characterisation of the surface structure of 3D printed scaffolds for cell infiltration and surgical suturing. *Biofabrication*. 2016;8(1):015016.
58. Declercq HA, Desmet T, Berneel EEM, Dubruel P, Cornelissen MJ. Synergistic effect of surface modification and scaffold design of bioplotting 3-D poly- ϵ -caprolactone scaffolds in osteogenic tissue engineering. *Acta Biomaterialia*. 2013;9(8):7699-708.

59. Beresford JN, Gallagher JA, Poser JW, Russell RG. Production of osteocalcin by human bone cells in vitro. Effects of 1,25(OH)₂D₃, 24,25(OH)₂D₃, parathyroid hormone, and glucocorticoids. *Metabolic bone disease & related research*. 1984;5(5):229-34.
60. Mosmann T. Rapid colorimetric assay for cellular growth and survival: application to proliferation and cytotoxicity assays. *J Immunol Methods*. 1983;65(1-2):55-63.
61. Livak KJ, Schmittgen TD. Analysis of relative gene expression data using real-time quantitative PCR and the 2⁻(-Delta Delta C(T)) Method. *Methods*. 2001;25(4):402-8.
62. Serra T, Planell JA, Navarro M. High-resolution PLA-based composite scaffolds via 3-D printing technology. *Acta Biomater*. 2013;9(3):5521-30.
63. Zein I, Hutmacher DW, Tan KC, Teoh SH. Fused deposition modeling of novel scaffold architectures for tissue engineering applications. *Biomaterials*. 2002;23(4):1169-85.
64. Wintermantel E, Mayer J, Blum J, Eckert KL, Luscher P, Mathey M. Tissue engineering scaffolds using superstructures. *Biomaterials*. 1996;17(2):83-91.
65. Raffaini G, Ganazzoli F. Surface topography effects in protein adsorption on nanostructured carbon allotropes. *Langmuir : the ACS journal of surfaces and colloids*. 2013;29(15):4883-93.
66. Li L, Qian Y, Jiang C, Lv Y, Liu W, Zhong L, et al. The use of hyaluronan to regulate protein adsorption and cell infiltration in nanofibrous scaffolds. *Biomaterials*. 2012;33(12):3428-45.
67. Oliveira JM, Silva SS, Malafaya PB, Rodrigues MT, Kotobuki N, Hirose M, et al. Macroporous hydroxyapatite scaffolds for bone tissue engineering applications: Physicochemical characterization and assessment of rat bone marrow stromal cell viability. *Journal of Biomedical Materials Research Part A*. 2009;91A(1):175-86.
68. Koroleva A, Deiwick A, Nguyen A, Schlie-Wolter S, Narayan R, Timashev P, et al. Osteogenic differentiation of human mesenchymal stem cells in 3-D Zr-Si organic-inorganic scaffolds produced by two-photon polymerization technique. *PloS one*. 2015;10(2):e0118164.
69. Gastman BR. Apoptosis and its clinical impact. *Head Neck*. 2001;23(5):409-25.
70. Pati F, Song TH, Rijal G, Jang J, Kim SW, Cho DW. Ornamenting 3D printed scaffolds with cell-laid extracellular matrix for bone tissue regeneration. *Biomaterials*. 2015;37:230-41.